

A FAST AND RIGOROUS CAD PROCEDURE FOR COMPLEX SHIELDED PLANAR CIRCUITS

George V. Eleftheriades, Hervé Le Pezennec, and Juan R. Mosig

Laboratoire d'Electromagnetisme et d' Acoustique  
Ecole Polytechnique Fédérale de Lausanne  
Lausanne, CH-1015, Switzerland

ABSTRACT

An efficient Integral-Equation/Method of Moments (MoM) technique is presented for the analysis of shielded planar circuits (MIC's and MMIC's). Unlike traditional approaches which implicate the Fast Fourier Transform (FFT) to compute the slowly converging MoM matrix elements, this technique is not restricted to uniform meshes. This feature is exploited by introducing a new modular meshing strategy with rectangular cells. The entire formulation is extended to multilayer/multiconductor substrates.

INTRODUCTION

The main obstacle towards the development of efficient Moment Method (MoM) techniques for shielded planar circuits stems from the excessive CPU time required to fill the corresponding impedance matrices [1]-[5]. The most widely adopted solution to this problem is to use the Fast Fourier Transform (FFT) in order to rapidly sum the involved 2D sinusoidal series [1]-[2]. Unfortunately, the FFT restricts the underlying discretization to uniform meshes. This can introduce redundant unknowns and hinders the accurate description of the circuit geometries.

Recently, a new technique has been proposed for significantly reducing the MoM matrix filling time even in the case of non-uniform meshes [4]-[5]. The technique begins by extracting the asymptotic part of the 2D box Green's function modal summation. This allows to separate the MoM matrix into Frequency-Dependent (FD) and Frequency-Independent (FI) parts. Subsequently, the convergence of the remainder (FI) sum is accelerated by means of an integral transformation. The original formulation is now extended to multilayer/multiconductor shielded substrates based on the equivalent transmission-line representation of the multilayer Green's functions. The entire process drastically reduces the overall CPU time.

In the original work [4]-[5], the implemented MoM is based on a non-uniform global rectangular mesh which is constructed using unequally spaced parallel vertical and horizontal lines [6]. Although this kind of a mesh is much more flexible than the uniform one required by the FFT, it still imposes certain undesirable discretization limitations. Here, we present a new strategy for creating the non-uniform rectangular mesh which offers significant flexibility over [4]-[6] and leads to faster and more accurate numerical results. The new strategy is based on a modular approach in which the circuit-geometry is partitioned into locally-discretized elementary rectangular objects.

SUMMARY OF THE FORMULATION

The general structure considered consists of passive printed circuits on a shielded multilayer isotropic substrate, as shown in Fig. 1. The corresponding Integral-Equation for the planar currents  $\vec{J}_s$  is given by [4]-[7]:

$$\hat{z} \times \vec{E}_{inc} = \hat{z} \times \left[ j\omega \int_s \vec{G}_A \cdot \vec{J}_s ds' - \frac{\nabla}{j\omega} \int_s G_v \nabla \cdot \vec{J}_s ds' + Z_s \vec{J}_s \right] \quad (1)$$

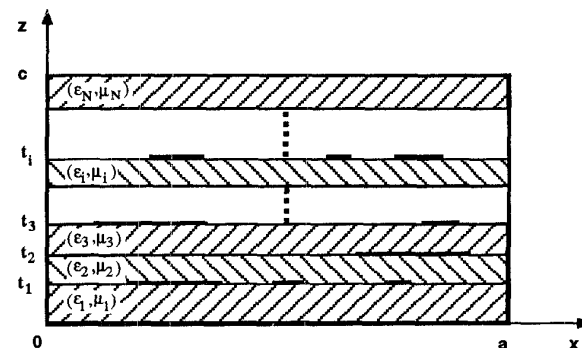


Fig.1: The multilayer/multiconductor substrate enclosed in a rectangular (box) cavity (axbxc).

The associated potential dyadic Green's functions for  $\hat{x}$ -directed currents are [4]-[5]:

TH  
2E

$$G_A^{xx} = \sum_{m=0}^{\infty} \sum_{n=0}^{\infty} \frac{j\epsilon_{0m}\epsilon_{0n} V_{mn}^{TE}(z, z', \omega)}{ab\omega} \cos\left(\frac{m\pi x'}{a}\right) \cos\left(\frac{m\pi x}{a}\right) \sin\left(\frac{n\pi y}{b}\right) \sin\left(\frac{n\pi y'}{b}\right) \quad (2)$$

$$G_V = \sum_{m=1}^{\infty} \sum_{n=1}^{\infty} \frac{4j\omega}{abK_{mn}^2} \left[ V_{mn}^{TE}(z, z', \omega) - V_{mn}^{TM}(z, z', \omega) \right] \sin\left(\frac{m\pi x'}{a}\right) \sin\left(\frac{m\pi x}{a}\right) \sin\left(\frac{n\pi y}{b}\right) \sin\left(\frac{n\pi y'}{b}\right) \quad (3)$$

where the coefficients  $V_{mn}^{TE}(z, z', \omega)$ ,  $V_{mn}^{TM}(z, z', \omega)$  represent voltages on equivalent transmission lines for each  $TE_z / TM_z$  waveguide mode [8]. In order to accelerate the computation of the double summations (2) and (3), we introduce the (FI) asymptotic components of the potential Green's function  $\hat{G}_A^{xx, TE}, \hat{G}_V^{TE}, \hat{G}_V^{TM}$  as described in [4]-[5]. These "caret" components are obtained by the asymptotic evaluation of  $V_{mn}^{TE}(z, z', \omega)$ ,  $V_{mn}^{TM}(z, z', \omega)$  as the indexes  $m, n$  tend to infinity. Subsequently, the asymptotic components are added and subtracted to equations (2), (3) resulting to Kummer's series acceleration method [9]. Finally, the convergence of the slowly-convergent (FI) components  $\hat{G}_A^{xx, TE}, \hat{G}_V^{TE}, \hat{G}_V^{TM}$  is enhanced by a suitable integral transformation technique.

Equations (4) and (5) describe the transformed (FI) TM part of the scalar potential Green's function for Fig.1 :

$$\hat{G}_V^{TM}(z, z') = \begin{cases} \sum_{m=1}^{\infty} -\frac{\sin\left(\frac{m\pi x'}{a}\right) \sin\left(\frac{m\pi x}{a}\right)}{ab\epsilon_f(z')} S_m^{(1)}, & z = z' \\ 0, & \text{otherwise} \end{cases} \quad (4)$$

$$S_m^{(1)} = \frac{2b}{\pi} \sum_{n=-\infty}^{\infty} \left\{ K_0\left(\frac{m\pi}{a}(y - y' + 2nb)\right) - K_0\left(\frac{m\pi}{a}(y + y' + 2nb)\right) \right\} \quad (5)$$

where  $\epsilon_f(z') = \epsilon_i + \epsilon_{i+1}$  and  $\epsilon_i, \epsilon_{i+1}$  are the permittivities of the two layers adjacent to the source interface at  $z'$ . Note that, due to the presence of the fast-decaying modified Bessel function  $K_0$ , only 2-3 terms suffice in (5) to achieve convergence. Equations (4)-(5) imply that the asymptotic interaction between the observation and source points  $(z, z')$  vanishes when they do not lie on the same interface. To the same degree of asymptotic approximation, when the points  $(z, z')$  do lie on the same interface, no reflections arrive at  $z = z'$  from any other interface. Although asymptotics that partially account for layer reflections can easily be constructed [10], it is judged that equations (4)-(5) lead to the best compromise between speed and algorithmic robustness.

For the (FD) computations, the required voltage coefficients are computed recursively based on a specially adapted reflection-coefficient approach [8]. As a consequence, only exponentials of negative arguments are evaluated for evanescent modes, thus ensuring overall numerical stability.

## MESHING STRATEGY AND RESULTS

Consider the geometry of Fig. 2.a which can be encountered, for example, as a part of an interdigital filter. The horizontal fingers are deliberately chosen of slightly different lengths, a situation which is not uncommon in practice. When the global meshing strategy with horizontal and vertical parallel lines is attempted [4]-[6], very fine vertical mesh lines appear at the open ends of the fingers, as shown in Fig. 2.b. This unnecessarily fine discretization can cause numerical problems and strain the entire computational effort.

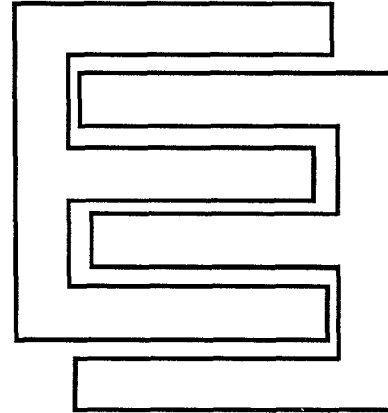


Fig. 2.a An example circuit geometry for which a global-mesh becomes inefficient (see text).

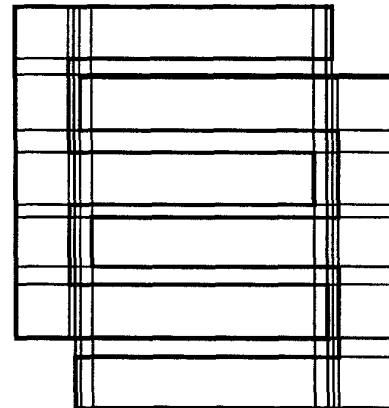


Fig. 2.b The obligatory mesh-lines for a grid of non-uniformly spaced horizontal & vertical parallel lines.

To overcome this type of problems, we adopt here a different, *modular*, meshing strategy: First, the global geometry is divided into elementary rectangular objects as shown in Fig. 3.a and with the associated topological object connectivity information stored in an appropriate matrix. The challenge now is to discretize each object individually but at the end to ensure that local meshes conform to each other. For this purpose, before starting the individual meshing process, a set of possible *constraint nodes* (CN) is identified on the perimeters of the objects. The (CN) set consists of two nodal subsets, the direct (CNd) and the indirect (CNi) subsets of nodes. The (CNd) are vertices which lie on the sides of other objects as denoted with black dots in Fig. 3.a. The (CNi) nodes arise as a consequence of using rectangular cells and rooftop basis functions: In this case, each (CNd) node introduces one vertical and another horizontal *obligatory* mesh lines, which are traversed until an object is encountered that is not directly connected to the previous one. In this manner, the (CNi) nodes are identified as marked with crosses in Fig. 3.a. Subsequently, the perimeter of each object is meshed individually based on the (CN) and on the desired discretization step  $\Delta$  ( $1/\Delta$ =cells-per-wavelength). In this way, all common object sides are *uniquely* partitioned. The final result of the new meshing strategy for the example under consideration, is illustrated in Fig. 3.b. The flexibility of the proposed strategy becomes apparent when comparing Fig. 3.b with Fig. 2.b.

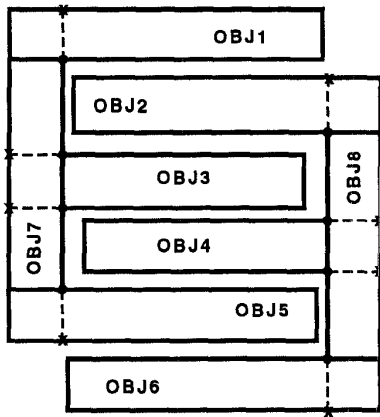


Fig. 3.a The circuit geometry of Fig. 2.a when divided into rectangular objects and the associated constraint nodes (CNd denoted by dots, CNi denoted by crosses).

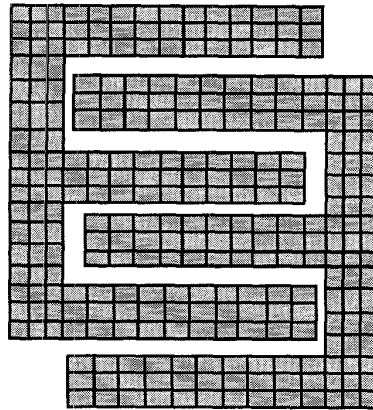


Fig. 3.b The result of the new meshing strategy.

The entire CAD procedure is being implemented on a HP9000/730 workstation. As a demonstration we present in Fig. 4, a simple shielded notch filter which is meshed according to the above modular strategy. The corresponding simulated and measured results are presented in Figures 5.a and 5.b for the magnitude and phase of the insertion loss, respectively.

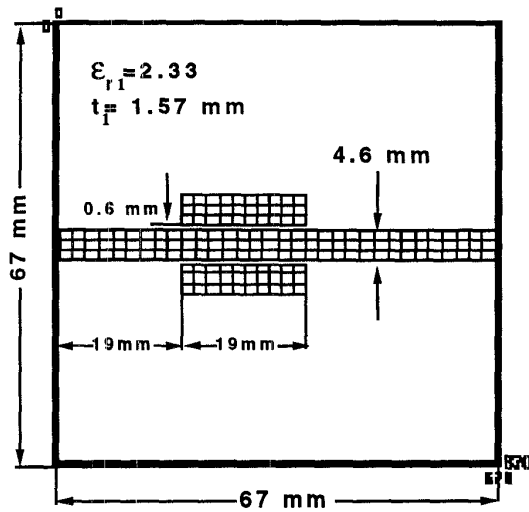


Fig. 4: A three coupled-line notch filter in a box of 67X67X11.4 mm and the associated mesh.

## ACKNOWLEDGMENT

This work has been supported by the European Space Technology Center (ESTEC), Noordwijk, the Netherlands, under contract No. A0/1-2742/94/NL/NB.

## REFERENCES

- [1] J.C. Rautio and R.F. Harrington, "An electromagnetic time-harmonic analysis of shielded microstrip circuits", *IEEE Trans. Microwave Theory Tech.*, vol. MTT-35, pp. 726-730, Aug. 1987.
- [2] A. Hill and V.K. Tripathi, "An efficient algorithm for the three dimensional analysis of passive components and discontinuities for microwave and millimeter wave integrated circuits", *IEEE Trans. Microwave Theory Tech.*, vol. 39, pp. 83-91, Jan. 1991.
- [3] L.P. Dunleavy and P.B. Katehi, "A generalized method for analyzing thin microstrip discontinuities", *IEEE Trans. Microwave Theory Tech.*, vol. 36, pp. 1758-1766, Dec. 1988.
- [4] G.V. Eleftheriades, J.R. Mosig and M. Guglielmi, "An efficient mixed potential integral equation technique for the analysis of shielded MMIC's", *Proceedings of the 25th European Microwave Conference*, pp. 825-829, Sept. 1995.
- [5] G.V. Eleftheriades, J.R. Mosig, and M. Guglielmi, "A fast integral equation technique for shielded planar circuits defined on non-uniform meshes." Submitted for publication to the *IEEE Trans. on Microwave Theory and Techniques*.
- [6] A. Skrivervik and J.R. Mosig, "Equivalent circuits of microstrip discontinuities including radiation effects," *IEEE MTT-S Int. Microwave Symp. Dig.*, pp. 1147-1150, 1989.
- [7] G.V. Eleftheriades and J.R. Mosig, "On the network characterization of planar passive circuits using the method of moments". To appear in the *IEEE Trans. Microwave Theory and Techniques*, March 1996.
- [8] L.B. Felsen and N. Marcuvitz, *Radiation and Scattering of Waves*, Prentice-Hall, Englewood Cliffs, N.J., pp. 185-217, 1973.
- [9] K. Knopp, *Theory and Application of Infinite Series*, Dover, New York, NY, 1990.
- [10] R.E. Collin, *Foundations of Microwave Engineering*, McGraw-Hill, New York, NY, pp. 224-237, 1966.

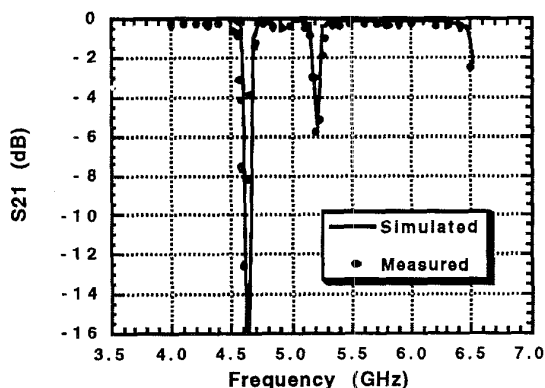


Fig. 5.a The computed and measured magnitude of the insertion loss. The first dip at 4.62 GHz is due to a box resonance while the second at 5.2 GHz is due to the circuit.

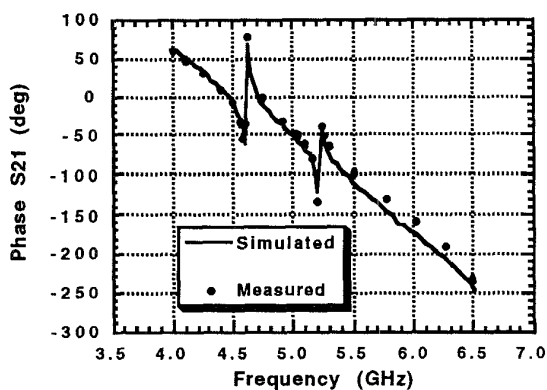


Fig. 5.b The computed and measured phase of the insertion loss.

## CONCLUSION

An efficient and rigorous CAD procedure has been presented for shielded planar circuits on multilayer substrates (MIC's and MMIC's). Unlike traditional MoM approaches for this class of problems, the underlying computational technique remains efficient even for non-uniform meshes. This feature is exploited by introducing a new modular meshing strategy with rectangular cells. Due to its modularity, the strategy can naturally be generalized to meshes consisting of both rectangular and triangular cells. This can lead to a CAD procedure for shielded MMIC's which combines maximum discretization flexibility together with high computational efficiency.